

See discussions, stats, and author profiles for this publication at: <https://www.researchgate.net/publication/265048564>

# Preparation of polyelectrolyte/calcium phosphate hybrids for drug delivery application

ARTICLE *in* CARBOHYDRATE POLYMERS · NOVEMBER 2014

Impact Factor: 4.07 · DOI: 10.1016/j.carbpol.2014.07.022

---

CITATIONS

5

---

READS

78

2 AUTHORS, INCLUDING:

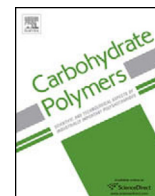


[Mohamed El-Sakhawy](#)

National Research Center, Egypt

47 PUBLICATIONS 438 CITATIONS

SEE PROFILE



# Preparation of polyelectrolyte/calcium phosphate hybrids for drug delivery application



Ahmed Salama\*, Mohamed El-Sakhawy

Cellulose and Paper Department, National Research Center, El-Tahrir Street, Dokki, Cairo, Egypt

## ARTICLE INFO

### Article history:

Received 27 March 2014

Received in revised form 12 June 2014

Accepted 2 July 2014

Available online 31 July 2014

### Keywords:

Hybrid

Polyelectrolyte

Drug delivery

Carboxymethyl cellulose

Chitosan

Calcium phosphate

## ABSTRACT

Biocompatible and biodegradable polyelectrolyte complex consisting of carboxymethyl cellulose (CMC) and chitosan (CHI) were studied as a template for calcium phosphate biomimetic mineralization. CMC/CHI/calcium phosphate hybrids were prepared using different concentrations of simulated body fluid (2, 5 and  $10 \times$  SBF) for producing hybrids with different organic/inorganic ratio. These hybrids were characterized using X-ray diffraction (XRD), infrared spectroscopy (FT-IR), thermogravimetric analysis (TGA), Scanning electron microscopy (SEM) and energy dispersive X-ray spectroscopy (EDX). The equilibrium swelling extents of the hybrids were found to be dependent on the inorganic % in the hybrids. The release profile of bovine serum albumin as a model drug in simulated intestine solution (pH 7.4) during 24 h has established the efficiency of the hybrids as a sustained delivery system. The hybrids developed in this contribution exhibit a great potential in bone tissue engineering and drug delivery applications.

© 2014 Elsevier Ltd. All rights reserved.

## 1. Introduction

Recently, the combination of ceramic particles with polymeric matrices has been extensively investigated as an alternative in bone tissue engineering (Danilchenko et al., 2011; Schweizer & Taubert, 2007). This process attempt to mimic the formation of mineralized tissues which composed of hierarchically neat apatite with collagen. It is reported that, the organized structures of bone have been shown to form by nonclassical mineralization processes controlled by polyelectrolyte rich in acidic moieties (Ye, Wang, Zeiger, Miles, & Lin-Gibson, 2013). Moreover, it is highly desirable that hybrid materials can be used for bone implantation and drug delivery synergistically (Zhang & Zhang, 2002). Using simulated body fluid (SBF) with ion concentrations nearly equal to those of human blood plasma requires more than 7 days for producing a uniform apatite coatings. However, using SBF with high ionic concentrations have been cited as a method to control the surface topography in biomimetic calcium phosphate mineralization and to reduce the time required for biomimetic mineralization process (Costa et al., 2012). Practically, several studies have been made to understand the interactions between charged polymers and calcium phosphate to better control the biomimetic mineralization process. Moreover, a number of acidic molecules such as

polyaspartic acid (Deshpande & Beniash, 2008) and polyacrylic acid (Liu et al., 2011) have been shown to promote intrafibrillar mineralization. These acidic polymers exhibit differences in their ability to control the mineralization process. Recently, the kinetics of calcium phosphate aggregation in the presence of carboxylate-bearing polymers has been studied. The results revealed that the polymer structure can alter calcium phosphate aggregation mechanisms, whereas polymer concentration influences the rate of calcium phosphate aggregation (Ye et al., 2013). However, using natural polymers in biomimetic mineralization, especially anionic polysaccharide, are a new approach for those purposes. Attempts have been carried out to enhance calcium phosphate mineralization onto ionic polysaccharides for preparation of hybrid materials resemble natural bone although it have different chemical structure (Barbosa, Granja, Barrias, & Amaral, 2005; Liuyun, Yubao, & Chengdong, 2009). In addition, using natural polymers as scaffolds for tissue engineering prevents the risks which may occur due to morbidity between human cells and scaffolds. The biodegradability of these polymers prevents a second surgical procedure for removing the scaffold after bone healing. However, there are only a few reports on the synthesis of carbohydrate/calcium phosphate hybrid materials. For example, Coleman and coworkers studied the rate of hydroxyapatite growth and mineralization using anionic polysaccharides like alginate and phosphorylated alginate. They found that alginate had no large effect on development of calcium phosphate crystals comparing to phosphorylated alginate which exhibited strong non-specific binding to the crystals (Coleman, Jack, Perrier, & Grøndahl,

\* Corresponding author. Tel.: +20 1008842629.

E-mail address: [ahmed\\_nigm78@yahoo.com](mailto:ahmed_nigm78@yahoo.com) (A. Salama).

2013). Sotome et al. (2004) prepared hydroxyapatite/collagene-alginate as bone filler and as a carrier for drugs. This hybrid was implanted into the femur and the results showed high bone formation, stability against enzyme digestion comparing with the same hybrid without alginate. Wang et al. prepared calcium phosphate/carboxymethyl chitosan hybrid materials nanoparticles by precipitation method for doxorubicin hydrochloride delivery. The hybrid materials loaded with drug were decorated by peptide KALA via self-assembly method. The in vitro study of these decorated nanoparticles shows that the cell inhibition significantly enhanced by the presence of peptide (Wang et al., 2013).

Carboxymethyl cellulose (CMC), the major commercial derivative of cellulose, is anionic polysaccharide widely used in pharmaceuticals (Devi & Maji, 2009) and in biomedical fields (Ninan et al., 2013; Rodríguez, Rennecker, & Gatenholm, 2011). A three dimensional carboxymethyl cellulose/hydroxyapatite nanocomposites were investigated for their application as a load bearing synthetic bone graft. The study showed that ionic/polar or electrostatic interactions are the main driving force for formation of load bearing three dimensional nanocomposites via a process similar to matrix mediated biomineralization (Garai & Sinha, 2013).

Chitosan (CHI) is the nature unique cationic polysaccharide composed of  $\beta$ -(1,4)-linked glucosamine that is produced via the alkaline deacetylation of chitin, the second-most abundant natural polymer after cellulose (Chicaturu et al., 2011). CHI has numerous and plentiful amino and hydroxyl groups in the macromolecular chains which provide advantageous for conducting medications reactions and for providing distinctive biological functions (Danilchenko et al., 2011). Accordingly, CHI has been studied for a wide range of biomedical applications such as drug delivery (Hu, Yang, & Hu, 2011; Wang et al., 2010) and tissue engineering as a scaffolding material (Rinaudo, 2008) because its degradation accompanied without inflammatory reactions or toxic products (Chen et al., 2009). Moreover, CHI has the ability to promote growth and mineral rich matrix in cell culture and osteoconductivity (Tanase, Popa, & Verestiuc, 2012).

Polyelectrolytes are mixtures of positively and negatively charged polymers blended at the molecular level (Sun, An, Zhao, Shangguan, & Zheng, 2012). Polyelectrolytes were reported as stimulated materials for inorganic biomimetic mineralization like  $\text{CaCO}_3$ ,  $\text{BaSO}_4$  and hydroxyapatite (Sun et al., 2012). Polyelectrolytes have been developed to be used as guide bone tissue regeneration. CMC can interact strongly with CHI due to the structural similarity. Consequently, CMC/CHI polyelectrolyte was widely investigated in the field of biomaterials (Chen & Fan, 2007; Jiang et al., 2008; Liuyun et al., 2009).

The current article focuses on the development of biodegradable porous scaffolds made from naturally derived polymers. CMC and CHI were chosen because their composition exhibits virtually no endotoxicity, cytotoxicity, and no antigenic properties upon implantation. The biomimetic mineralization process of polyelectrolyte could be enhanced using high concentrations of simulated body fluids (SBF). The study also addresses the morphology, crystal phase of mineralized calcium phosphate on the swellable CMC/CHI polyelectrolyte's. Moreover, the release profile of bovine serum albumin, a model for macromolecules and drugs, as a function in inorganic ratio was investigated.

## 2. Materials and methods

### 2.1. Materials

Carboxymethyl cellulose sodium salt (>99.5%) with high viscosity (4% in water at 25 °C are 1000–1500 mPa S) was purchased from

**Table 1**

Compositions of 2×, 5× and 10× SBF.

		2×	5×	10×
Phosphate part <sup>a</sup> [gm]	Tris	1.2110	3.0275	6.055
	$\text{Na}_2\text{SO}_4 \cdot 10\text{H}_2\text{O}$	0.0644	0.161	0.322
	$\text{NaHCO}_3$	0.1411	0.3528	0.7055
	$\text{K}_2\text{HPO}_4$	0.0696	0.174	0.348
Calcium part [gm]	Tris	1.2110	3.0275	6.055
	$\text{NaCl}$	3.1980	7.995	15.99
	$\text{KCl}$	0.0880	0.22	0.44
	$\text{MgCl}_2 \cdot 6\text{H}_2\text{O}$	0.1220	0.305	0.61
	$\text{CaCl}_2 \cdot 2\text{H}_2\text{O}$	0.1470	0.3675	0.735

<sup>a</sup> Every part dissolves in 100 mL double distilled water.

Fluka Biochemika. Chitosan, microcrystalline molecular weight: 100 000 to 300 000 and deacetylating grade 70 to 85% was supplied from Acros. Comassie brilliant blue (G-250) and bovine serum albumin (BSA) were supplied by Sigma-Aldrich, St. Louis, USA. All other reagents were of analytical grade and used as received without further purification.

### 2.2. CMC/CHI polyelectrolyte complex preparation and mineralization

CMC (100 mg) was dissolved in 10 mL deionized water and CHI (100 mg) was dissolved in 10 mL 2% acetic acid solution. The two solutions were mixed 1:1 by adding the CMC drop wise into the stirring CHI solution. The formed polyelectrolyte was washed by deionized water to remove acetic acid residue and freeze dried.

Simulated body fluids with different concentrations were prepared as shown in Table 1, to accelerate the calcium phosphate formation (Ohtsuki, Kokubo, & Yamamuro, 1992). The biomimetic mineralization process by immersing 5 gm of swellable CMC/CHI polyelectrolytes in 50 mL (25 mL from each of calcium and phosphate part) 2×, 5× and 10× SBF in Falcon tubes for 72 h. The samples were attached by polystyrene thread to prevent the formation of calcium phosphate by precipitations. SBF was renewed after centrifugation every 24 h and the pH was checked on samples regularly. pH values were maintained at 7.4 over the entire course of the mineralization to minimize problems associated with SBF preparation and stabilization (Bohner & Lemaître, 2009). Finally, the samples were washed with double distilled water for 5 days and dried at room temperature for further analysis.

### 2.3. Characterization methodology

#### 2.3.1. ATR-FTIR

Attenuated total reflection-Fourier transform infrared spectroscopy (ATR-FTIR) was done on a Thermo Nicolet FT-IR Nexus 470 with a diamond crystal. Spectra were recorded from 500 to 4000  $\text{cm}^{-1}$  with a resolution of 2  $\text{cm}^{-1}$ .

#### 2.3.2. XRD

X-ray diffraction (XRD) patterns were recorded using a Philips apparatus PW 105 diffractometer (Philips Analytical, Cambridge, UK) using Ni-filtered Cu radiation ( $\text{CuK}\alpha$ , 0.154 nm) at an operating voltage of 40 kV.

#### 2.3.3. SEM and EDX

Scanning electron microscopy was done on a JEOL JXA-840A Electron probe microanalyzer with tungsten filament (30 kV). For EDX experiments an Oxford INCAx-sight SN detector with a resolution of 128 eV at 5.9 keV was used.

### 2.3.4. Thermogravimetric analysis (TGA)

Thermogravimetric analysis was done on a Linseis STA PT-1600 thermal balance in air from 20 to 600 °C with a heating rate of 10 K min<sup>-1</sup> and air flow of 50 mL min<sup>-1</sup>.

### 2.4. Equilibrium water absorbance of CMC/CHI pure and mineralized polyelectrolyte

The equilibrium swelling of the CMC/CHI polyelectrolyte and the calcium phosphate/polyelectrolyte hybrids were investigated in pH similar to that of physiological fluid (7.4). The buffer solution composed of phosphoric acid (0.054 mol), boric acid (0.040 mol) and acetic acid (0.042 mol) and then adjusted to the required pH value by the dropwise addition of 0.2 N NaOH solution. A preweighed hybrids were immersed in 20 mL of buffer solution and the swollen hybrids weights were determined after removal of the surface liquid using tissue paper, until equilibrium swelling was attained. The swelling percent was calculated by the following equation:

$$\text{Swelling\%} = \left[ \frac{(W_t - W_0)}{W_0} \right] \times 100$$

where  $W_0$  is the initial weight and  $W_t$  the weight of the hybrids at time  $t$ .

### 2.5. In-vitro BSA release

BSA-loaded polyelectrolyte/calcium phosphate hybrids were prepared by hybrids incubation in glass vials with 5 mL BSA solution (25 mg mL<sup>-1</sup>) for 48 h. After drying in vacuum oven, the amount of loaded drug was calculated. The hybrids were transferred to a glass vials containing 10 mL simulated intestinal fluids (pH 7.4) and incubated at 37 °C without stirring. After that, one milliliter of the release medium was taken periodically and assayed by Bradford method (Bradford, 1976) at  $\lambda_{\text{max}}$  595 nm using a photometer 5010 (Germany). The withdrawn medium was replaced with the same volume of buffer solution, to keep the volume of the release medium constant. The results were measured three times, and the average was recorded with standard deviation.

## 3. Results and discussion

The aim of the current study was to investigate the feasibility of the CMC/CHI polyelectrolyte polymer as a template for calcium phosphate mineralization. Bearing opposite charges, the combination of CMC and CHI via ionic interaction can form a polyelectrolyte complex in the form of hydrogel, the precursor for biomimetic mineralization process in this study. Moreover, the ionic interaction between two polymers avoids the use of organic precursors, catalysts, or cross-linking agents which alleviating the concern about toxicity or reactions with a therapeutic payload. Porous polyelectrolyte was examined under SEM after freeze drying which is desirable as no organic solvent residual traces are left behind.

### 3.1. Morphology and fiber-size distribution of CMC/CHI polyelectrolyte fibrous

Fig. 1 shows the surface topography of the microporous CMC/CHI 3D polyelectrolyte fibrous distribution which consisting of 50 wt% CMC and 50 wt% CHI. The polyelectrolyte presented a complete blend with a homogenous and a uniform fiber distribution. In addition, the polyelectrolyte fibrous had fiber diameter ranging from 0.5 to 2  $\mu\text{m}$  and pore size <5  $\mu\text{m}$ . It is regarded that surface roughness can enhance attachment and nucleation

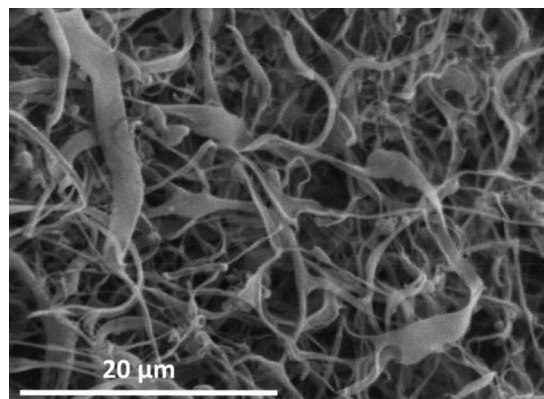


Fig. 1. SEM for CMC/CHI polyelectrolyte.

of calcium and phosphate ions for calcium phosphate growth layer.

### 3.2. IR

Polyelectrolyte CMC/CHI was incubated in a simulated body fluids with higher concentrations to those present in human blood plasma by 2 $\times$ , 5 $\times$  and 10 $\times$  for 72 h. FTIR spectra of pure and mineralized CMC/CHI polyelectrolyte at various SBF concentrations were presented in Fig. 2. The specific bands for both CMC and CHI appeared in the spectrum of the pure polyelectrolyte. The absorption bands at 3336 cm<sup>-1</sup> was attributed to stretching vibration of the N–H group and hydroxyl stretching vibrations. Moreover, absorption band at 1589 cm<sup>-1</sup>, corresponding to the characteristic bands of –NH<sup>3+</sup> and –COO<sup>-</sup>, which reflected strong electrostatic interaction between the negatively charged carboxylates (–COO<sup>-</sup>) on CMC and the positively charged amino groups (–NH<sup>3+</sup>) on CHI. However, the mineralized polyelectrolytes have a characteristic peaks at 1029 cm<sup>-1</sup> (P–O  $\nu_3$  mode), 561 cm<sup>-1</sup> (P–O  $\nu_4$  mode), and 890 cm<sup>-1</sup> (P–O  $\nu_1$  mode) which assigned to different vibrations modes of PO<sub>4</sub><sup>3-</sup> group in calcium phosphate.

### 3.3. XRD

The XRD patterns of the mineralized CMC/CHI hybrids at different SBF concentrations are displayed in Fig. 3. All hybrids exhibit a

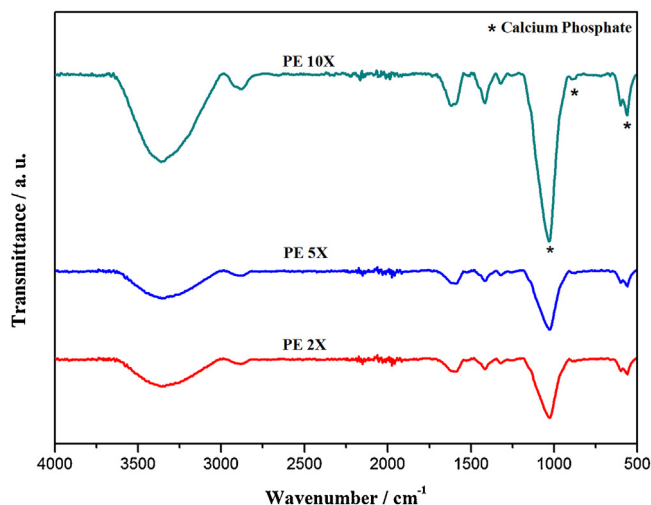
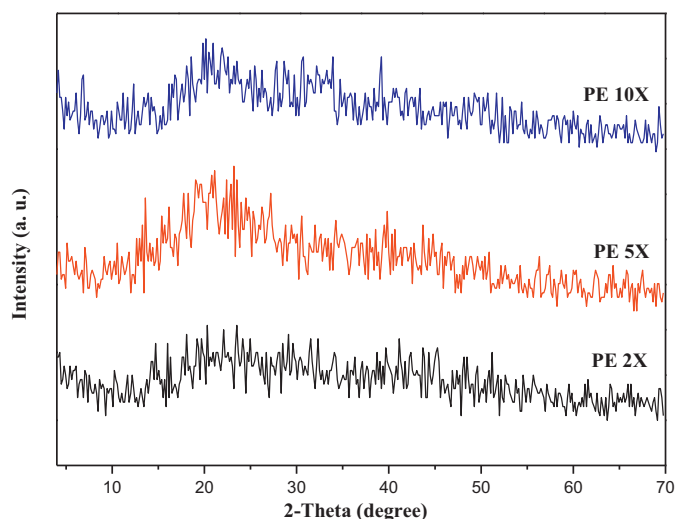


Fig. 2. FTIR spectra of pure (PE0) and mineralized CMC/CHI polyelectrolyte at different SBF concentrations (2 $\times$ , 5 $\times$  and 10 $\times$  SBF).



**Fig. 3.** XRD patterns of mineralized CMC/CHI hybrids at different concentrations of SBF.

very salient broad centered around  $2\theta$  of  $22^\circ$  which assigned to the amorphous glassy structure of the CMC/CHI polyelectrolyte. Moreover, the diffractogram of the mineralized polyelectrolytes show no distinct crystalline peaks which may refer to formation of amorphous calcium phosphate. It is well established that hydroxyapatite is formed in metastable aqueous solutions via a precursor phase, most commonly amorphous calcium phosphate. The precursor amorphous calcium phosphate hydrolyzes into the more thermodynamically stable hydroxyapatite in aqueous solution at a pH greater than 4.2.

### 3.4. Thermogravimetric analysis

CMC/CHI polyelectrolyte and mineralized hybrid samples formed in different concentrations of SBF were subjected to thermogravimetric analysis to estimate the thermal stability and the actual content of the mineralized calcium phosphate. The thermogram assigned three ranges of mass loss of the polyelectrolyte/calcium phosphate samples (Yusufoglu et al., 2008). Removal of physically and chemically adsorbed water showed initial smooth weight loss started from room temperature up to  $200^\circ\text{C}$ . The main weight loss decomposition occurred between 200 and  $400^\circ\text{C}$  which could be associated with CMC and CHI pyrolysis including depolymerization, dehydration, and decomposition of glucosyl units (Saska et al., 2011). At approximately  $500^\circ\text{C}$ , CMC/CHI polyelectrolyte has completely degraded and the inorganic phase (calcium phosphate) still remains. If calcium phosphate has some incorporated carbonate in the form of carbonated apatite, there will be a weight loss above  $400^\circ\text{C}$  due to the CO removal from the hydroxyl apatite structure (Yusufoglu & Akinc, 2008). A slight mass loss between the temperature ranges of  $400$ – $600^\circ\text{C}$  (Fig. 4) possibly corresponds to the decarboxylation of the calcium phosphate. The analyses of Fig. 4 and Table 2 show that increasing the concentration of SBF from  $2\times$  to  $5\times$  or  $10\times$  was accompanied with an inorganic residue increase from 7.30 to 17.35 and 38.57,

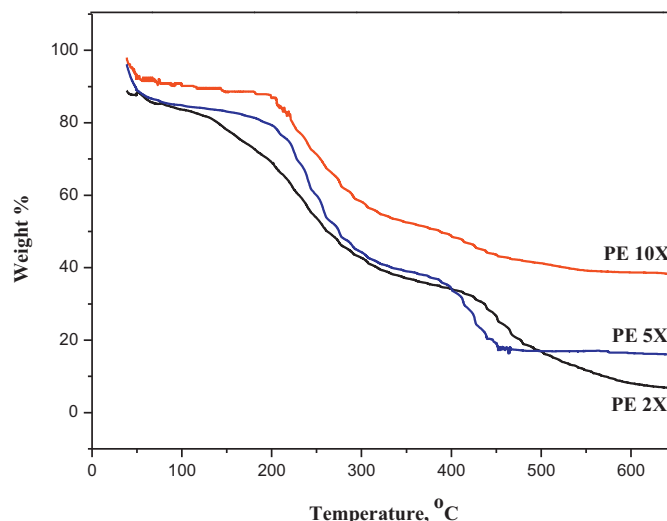


**Fig. 4.** TGA for pure and mineralized polyelectrolyte.

respectively. Fig. 4 also shows the increasing of the hybrids thermal stability with increasing the mineral content which clearly demonstrates that the mixing between the polyelectrolyte organic polymers and mineralized calcium phosphate is on the molecular level.

### 3.5. SEM and EDX

Morphologies of calcium phosphate synthesized at high ion concentrations ( $2\times$ ,  $5\times$  and  $10\times$  SBF) are observed in Fig. 5. As shown, polyelectrolyte fibrous incubated in  $2\times$  SBF were covered with heterogeneous and sparsely dispersed spherically-shaped particles after 72 h of incubation. Moreover, the rate of growth and the size of calcium phosphate spherical globules were found to increase remarkably by increasing the ionic strength of the simulated body fluid. Hydrogen bonding between the organic polymer and the inorganic mineral plays an important role in avoiding phase separation and yielding homogenous free standing hybrid (Rangelova et al., 2011). The increasing of SBF to  $5\times$  greatly affected the growing process and the final morphology by forming more homogenous with large spherically-shaped particles of the precipitated calcium phosphate. In addition, these calcium phosphate layers became denser and completely filled the pores between polyelectrolyte fibrous at higher simulated body fluid concentration ( $10\times$ ). Thus, incubation of CMC/CHI polyelectrolyte in different concentrations of simulated body fluids can be used to produce calcium phosphate layer with different topographical features and different particles morphology which may refer to the formation of calcium phosphate with different phases.

The EDX analysis detected the presence of Ca and P elements as the major constituents with Ca/P ratio 1.42, 1.61 and 1.69 for polyelectrolyte  $2\times$ ,  $5\times$  and  $10\times$ , respectively. Moreover, EDX shows sharp increase in the Ca and P content on the surface of the hybrids, likely due to the consequence increase in SBF concentration. In addition, the Ca/P atomic ratios of the mineralized surfaces for

**Table 2**  
EDX and TGA data obtained for polyelectrolyte mineralized at different SBF concentrations.

Sample	SBF	EDX Atom%		Ca/P	TGA
		Ca	P		Weight loss at $600^\circ\text{C}$ [%] (residue)
PE2X	$2\times$	$12.72 \pm 0.45$	$8.98 \pm 0.31$	$1.42 \pm 0.01$	92.70 (7.30)
PE5X	$5\times$	$18.7 \pm 4.59$	$11.53 \pm 1.99$	$1.61 \pm 0.12$	82.65 (17.35)
PE10X	$10\times$	$26.66 \pm 2.33$	$16.35 \pm 1.94$	$1.69 \pm 0.05$	61.43 (38.57)



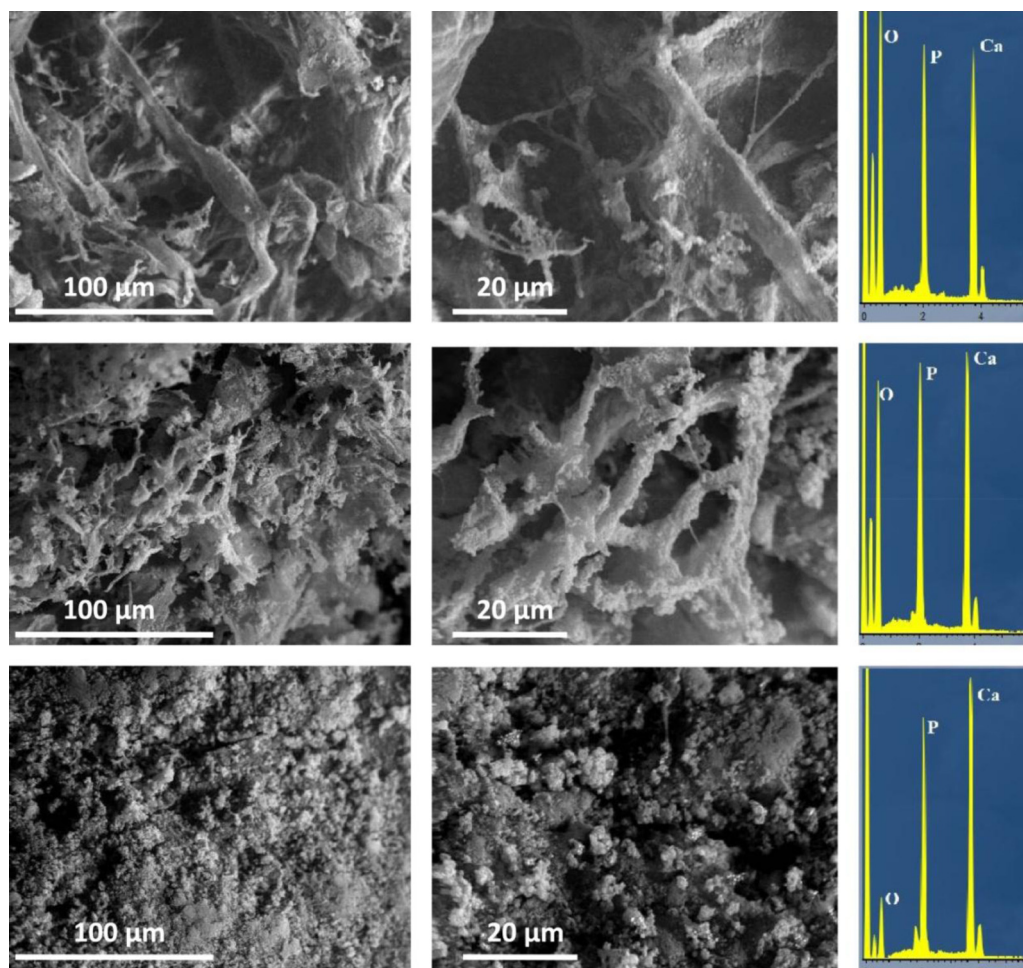


**Fig. 5.** SEM at different magnifications and representative EDX for polyelectrolyte/calcium phosphate hybrid mineralized in 2× (top row), 5× (middle row) and 10 × SBF (bottom row).

PE 2× (1.42) are below the stoichiometric value of 1.5 for amorphous calcium phosphate. PE 5× and 10× have Ca/P atomic ratios from 1.61 to 1.69 which below the stoichiometric value of 1.67 for hydroxyapatite. Deviation from the stoichiometric value are known in the literatures and may be due to cationic substitutions at the  $\text{Ca}^{2+}$  sites by  $\text{Mg}^{2+}$  or  $\text{Na}^{+}$  or anionic substitution at  $\text{PO}_4^{3-}$  sites by  $\text{CO}_3^{2-}$  or  $\text{HPO}_4^{2-}$  or a combination of these substitutions (Costa et al., 2012). In conclusion, increasing the SBF concentration had a significant effect on the Ca/P ratio of the calcium phosphate mineralized layer which in so far produce a hybrid materials with different organic/inorganic ratios. The results from SEM and EDX studies clearly confirmed that the hybrids have new surface enriched by Ca and P, which are the main constituents of HA.

### 3.6. Growth mechanism of calcium phosphate on CMC/chitosan hybrid

It is reported that, the driving force for calcium phosphate inducing crystals is not only precipitation of calcium phosphate salts but also the activity of anionic and cationic functional groups to start nucleation process (Shkilnyy et al., 2008). In most cases of calcium-phosphate salts mineralization, amorphous calcium phosphate was firstly formed as non-crystalline form, which have strong tendency to become hydroxyapatite by dissolution and recrystallization (Dentini et al., 2012). This study showed that CMC/CHI could be used as an effective template for biomimetic mineralization to

synthesize calcium phosphate with rough surface. The construction of polyelectrolyte and the subsequent biomimetic mineralization mechanism are illustrated in Fig. 6. Calcium phosphate layer formation onto the surface of the CMC/CHI polyelectrolyte was promoted by carboxylic acid groups which present in the form of charged functional carboxylate at pH 7.4 (Costa et al., 2012). These charged functional groups act as nucleation sites which attract  $\text{Ca}^{2+}$  ions on the polyelectrolyte surface. After that, combination of calcium and phosphate ions will take place on the surface of polyelectrolyte which in turns starts to form a nucleus of calcium phosphate. These nuclei are formed on the polyelectrolyte surface and grow into a dense calcium phosphate layer by additional precipitation of calcium and phosphate ions from the SBF.

### 3.7. Swelling and bovine serum albumin % release from polyelectrolyte and hybrid

Fig. 7 shows the swelling behavior of the polyelectrolyte and polyelectrolyte/calcium phosphate hybrids at pH 7.4 and 37 °C. The swelling% of CMC/CHI polyelectrolyte was slightly higher than polyelectrolyte/calcium phosphate hybrids. The combination of calcium phosphate/polyelectrolyte would inhibit the extension of the polymer chain and then suppress the swelling ratio (Shi, Qi, Du, Shi, & Cao, 2013). Moreover, the polyelectrolyte hybrids need more long time to attain the equilibrium swelling. The swelling property will affect the drug-release percentage of the hybrid composites.

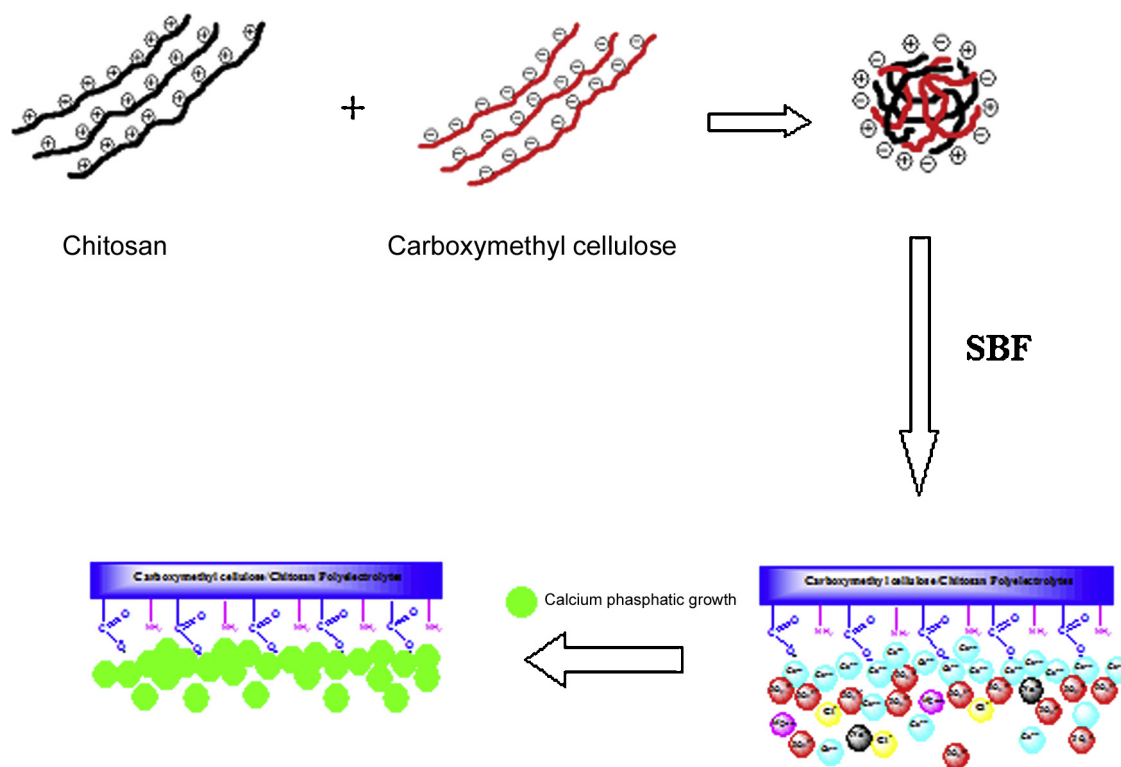


Fig. 6. Preparation of CMC/CHI polyelectrolyte hydrogel and biomimetic mineralization process using SBF.

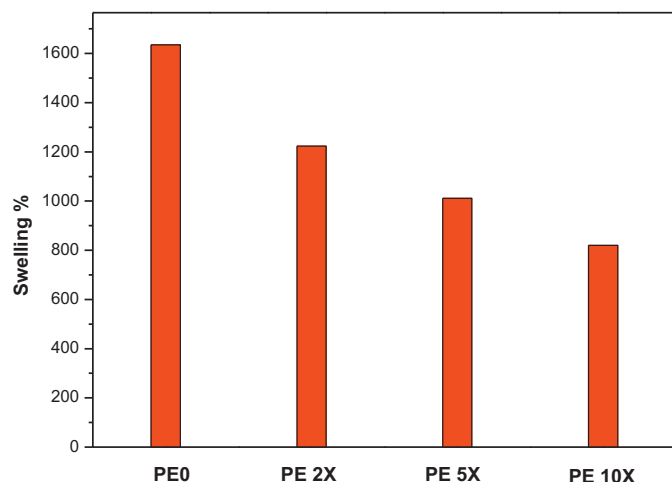


Fig. 7. Swelling % of pure CMC/CHI polyelectrolyte (PE0) and mineralized polyelectrolyte at different concentrations (2×, 5× and 10×) of SBF.

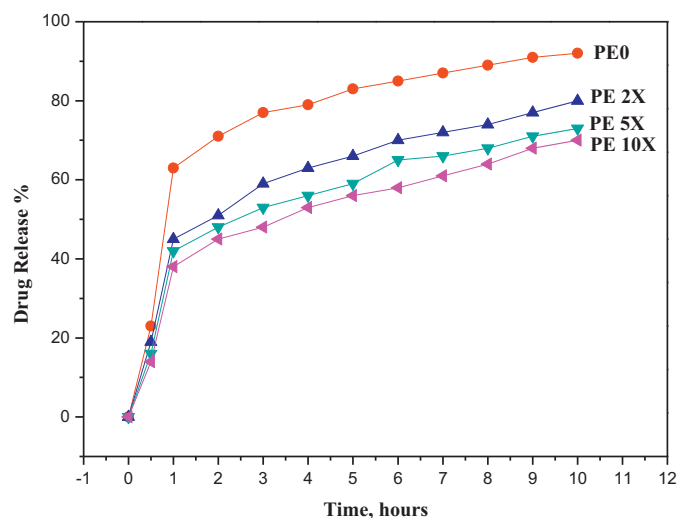


Fig. 8. Sustained BSA release profiles from pure CMC/CHI polyelectrolyte (PE0) and mineralized polyelectrolyte hybrids at different concentrations (2×, 5× and 10×) of SBF and pH 7.4.

Fig. 8 shows the BSA release profiles from CMC/CHI polyelectrolyte and mineralized polyelectrolyte hybrids prepared using different concentrations of SBF as crystal growth medium. The drug release was around 92% after 10 h for CMC/CHI polyelectrolyte. However, the release% for the hybrids prepared with 2×, 5× and 10× SBF were 80, 73 and 70%, respectively, at pH 7.4. It must be noted from Fig. 8 that the initial burst release of pure polyelectrolyte had been decreased after mineralization process. Moreover, the BSA release from the hybrid composites is in line with the morphology and swelling results. In addition, the release % slightly decreases with increasing the inorganic content. These results demonstrated that the mineralized polyelectrolyte could hinder the permeability of the encapsulated drug and reduce the drug release effectively.

#### 4. Conclusion

CMC/CHI polyelectrolyte hydrogel could be used as a template for calcium phosphate biomimetic mineralization. Polyelectrolyte/calcium phosphate hybrids synthesized in different concentrations of simulated body fluid solutions have different surface morphology and different organic/inorganic ratios. Thermogravimetric analysis showed an inorganic content of 7.3–38.57 wt% (based on the mass of the dried gel at around 600 °C) in the various samples. BSA release behaviors of the polyelectrolyte hybrid materials revealed sustained release properties from the calcium phosphate particles which hinder the permeation of the encapsulated drug. Mineralization within SBF solution

indicated that CMC/CHI polyelectrolyte hybrids could be made into a bioactive substrate that can be further studied for bone tissue engineering applications.

## Acknowledgment

This work was supported by the National Research Center in Cairo, Egypt. Project of cellulose and paper department (no. 10130101).

## References

- Barbosa, M. A., Granja, P. L., Barrias, C. C., & Amaral, I. F. (2005). Polysaccharides as scaffolds for bone regeneration. *ITBM-RBM*, 26, 212–217. <http://dx.doi.org/10.1016/j.rbmet.2005.04.006>
- Bohner, M., & Lemaître, J. (2009). Can bioactivity be tested in vitro with SBF solution? *Biomaterials*, 30(12), 2175–2179. <http://dx.doi.org/10.1016/j.biomaterials.2009.01.008>
- Bradford, M. M. (1976). A rapid and sensitive method for the quantitation of microgram quantities of protein utilizing the principle of protein-dye binding. *Analytical Biochemistry*, 72(1–2), 248–254. [http://dx.doi.org/10.1016/0003-2697\(76\)90527-3](http://dx.doi.org/10.1016/0003-2697(76)90527-3)
- Chen, H., & Fan, M. (2007). Chitosan/carboxymethyl cellulose polyelectrolyte complex scaffolds for pulp cells regeneration. *Journal of Bioactive and Compatible Polymers*, 22(5), 475–491. <http://dx.doi.org/10.1177/0883911507081329>
- Chen, K. Y., Liao, W. J., Kuo, S. M., Tsai, F. J., Chen, Y. S., Huang, C. Y., & Yao, C. H. (2009). Asymmetric chitosan membrane containing collagen I nanospheres for skin tissue engineering. *Biomacromolecules*, 10(6), 1642–1649. <http://dx.doi.org/10.1021/bm900238b>
- Chicautun, F., Pedraza, C. E., Ghezzi, C. E., Marelli, B., Kaartinen, M. T., McKee, M. D., & Nazhat, S. N. (2011). Osteoid-mimicking dense collagen/chitosan hybrid gels. *Biomacromolecules*, 12, 2946–2956.
- Coleman, R. J., Jack, K. S., Perrier, S., & Grøndahl, L. (2013). Hydroxyapatite mineralization in the presence of anionic polymers. *Crystal Growth & Design*, 13(10), 4252–4259. <http://dx.doi.org/10.1021/cg400447e>
- Costa, D. O., Allo, B. A., Klassen, R., Hutter, J. L., Dixon, S. J., & Rizkalla, A. S. (2012). Control of surface topography in biomimetic calcium phosphate coatings. *Langmuir*, 28(8), 3871–3880. <http://dx.doi.org/10.1021/la203224a>
- Danilchenko, S. N., Kalinkevich, O. V., Pogorelov, M. V., Kalinkevich, A. N., Sklyar, A. M., Kalinichenko, T. G., & Sukhodub, L. F. (2011). Characterization and in vivo evaluation of chitosan-hydroxyapatite bone scaffolds made by one step coprecipitation method. *Journal of Biomedical Materials Research A*, 96(4), 639–647. <http://dx.doi.org/10.1002/jbm.a.33017>
- Dentini, M., Barbeta, A., Ferrer, M. L., Monte, F., Chimica, D., Universita, S., & Moro, P. A. (2012). In Situ precipitation of amorphous calcium phosphate and ciprofl oxacin crystals during the formation of chitosan hydrogels and its application for drug delivery purposes. *Langmuir*, 28, 15937–15946.
- Deshpande, A. S., & Beniash, E. (2008). Bio-inspired synthesis of mineralized collagen fibrils. *Crystal Growth & Design*, 8(8), 3084–3090. <http://dx.doi.org/10.1021/cg800252f>
- Devi, N., & Maji, T. K. (2009). Preparation and evaluation of gelatin/sodium carboxymethyl cellulose polyelectrolyte complex microparticles for controlled delivery of isoniazid. *AAPS PharmSciTech*, 10(4), 1412–1419. <http://dx.doi.org/10.1208/s12249-009-9344-9>
- Garai, S., & Sinha, A. (2013). Biomimetic nanocomposites of carboxymethyl cellulose-hydroxyapatite: Novel three dimensional load bearing bone grafts. *Colloids and Surfaces B, Biointerfaces*, 115C, 182–190. <http://dx.doi.org/10.1016/j.colsurfb.2013.11.042>
- Hu, Y., Yang, T., & Hu, X. (2011). Novel polysaccharides-based nanoparticle carriers prepared by polyelectrolyte complexation for protein drug delivery. *Polymer Bulletin*, 68(4), 1183–1199. <http://dx.doi.org/10.1007/s00289-011-0683-9>
- Jiang, L., Li, Y., Wang, X., Zhang, L., Wen, J., & Gong, M. (2008). Preparation and properties of nano-hydroxyapatite/chitosan/carboxymethyl cellulose composite scaffold. *Carbohydrate Polymers*, 74(3), 680–684. <http://dx.doi.org/10.1016/j.carbpol.2008.04.035>
- Liu, Y., Li, N., Qi, Y., Dai, L., Bryan, T. E., Mao, J., & Tay, F. R. (2011). Intrafibrillar collagen mineralization produced by biomimetic hierarchical nanoapatite assembly. *Advanced Materials*, 23(8), 975–980. <http://dx.doi.org/10.1002/adma.201003882>
- Liuyun, J., Yubao, L., & Chengdong, X. (2009). A novel composite membrane of chitosan-carboxymethyl cellulose polyelectrolyte complex membrane filled with nano-hydroxyapatite. I. Preparation and properties. *Journal of Materials Science: Materials in Medicine*, 20(8), 1645–1652. <http://dx.doi.org/10.1007/s10856-009-3720-6>
- Ninan, N., Muthiah, M., Park, I.-K., Elain, A., Thomas, S., & Grohens, Y. (2013). Pectin/carboxymethyl cellulose/microfibrillated cellulose composite scaffolds for tissue engineering. *Carbohydrate Polymers*, 98(1), 877–885. <http://dx.doi.org/10.1016/j.carbpol.2013.06.067>
- Ohtsuki, C., Kokubo, T., & Yamamuro, T. (1992). Mechanism of apatite formation on CaSiO<sub>2</sub>P<sub>2</sub>O<sub>5</sub> glasses in a simulated body fluid. *Journal of Non-Crystalline Solids*, 143, 84–92. [http://dx.doi.org/10.1016/S0022-3093\(05\)80556-3](http://dx.doi.org/10.1016/S0022-3093(05)80556-3)
- Rangelova, N., Radev, L., Nenkova, S., Salvado, I. M. M., Fernandes, M. H. V., & Herzog, M. (2011). Methylcellulose/SiO<sub>2</sub> hybrids: sol-gel preparation and characterization by XRD, FTIR and AFM. *Central European Journal of Chemistry*, 9(1), 112–118. <http://dx.doi.org/10.2478/s11532-010-0123-y>
- Rinaudo, M. (2008). Main properties and current applications of some polysaccharides as biomaterials. *Polymer International*, 57(3), 397–430. <http://dx.doi.org/10.1002/pi.2378>
- Rodríguez, K., Rennecker, S., & Gatenholm, P. (2011). Biomimetic calcium phosphate crystal mineralization on electrospon cellulose-based scaffolds. *ACS Applied Materials & Interfaces*, 3(3), 681–689. <http://dx.doi.org/10.1021/am100972r>
- Saska, S., Barud, H. S., Gaspar, A. M. M., Marchetto, R., Ribeiro, S. J. L., & Messaddeq, Y. (2011). Bacterial cellulose-hydroxyapatite nanocomposites for bone regeneration. *International Journal of Biomaterials*, 2011, 175362. <http://dx.doi.org/10.1155/2011/175362>
- Schweizer, S., & Taubert, A. (2007). Polymer-controlled, bio-inspired calcium phosphate mineralization from aqueous solution. *Macromolecular Bioscience*, 7, 1085–1099. <http://dx.doi.org/10.1002/mabi.200600283>
- Shi, J., Qi, W., Du, C., Shi, J., & Cao, S. (2013). Micro/nanohybrid hierarchical poly (N-isopropylacrylamide)/calcium carbonate composites for smart drug delivery. *Journal of Applied Polymer Science*, 577–584. <http://dx.doi.org/10.1002/jp.38718>
- Shkilnyy, A., Friedrich, A., Tiersch, B., Schöne, S., Fechner, M., Koetz, J., & Taubert, A. (2008). Poly(ethylene imine)-controlled calcium phosphate mineralization. *Langmuir*, 24(5), 2102–2109. <http://dx.doi.org/10.1021/la702523p>
- Sotome, S., Uemura, T., Kikuchi, M., Chen, J., Itoh, S., Tanaka, J., & Shinomiya, K. (2004). Synthesis and in vivo evaluation of a novel hydroxyapatite/collagen-alginate as a bone filler and a drug delivery carrier of bone morphogenetic protein. *Materials Science and Engineering: C*, 24(3), 341–347. <http://dx.doi.org/10.1016/j.msec.2003.12.003>
- Sun, Z., An, Q., Zhao, Q., Shanguan, Y., & Zheng, Q. (2012). Study of polyelectrolyte complex nanoparticles as novel templates for biomimetic mineralization. *Crystal Growth & Design*, 12, 2382–2388.
- Tanase, C. E., Popa, M. I., & Verestiuc, L. (2012). Biomimetic chitosan-calcium phosphate composites with potential applications as bone substitutes: Preparation and characterization. *Journal of Biomedical Materials Research Part B: Applied Biomaterials*, 100B(3), 700–708. <http://dx.doi.org/10.1002/jbm.b.32502>
- Wang, J., Chen, B., Zhao, D., Peng, Y., Zhuo, R.-X., & Cheng, S.-X. (2013). Peptide decorated calcium phosphate/carboxymethyl chitosan hybrid nanoparticles with improved drug delivery efficiency. *International Journal of Pharmaceutics*, 446(1–2), 205–210. <http://dx.doi.org/10.1016/j.ijpharm.2013.02.028>
- Wang, J., Chen, J.-S., Zong, J.-Y., Zhao, D., Li, F., Zhuo, R.-X., & Cheng, S.-X. (2010). Calcium carbonate/carboxymethyl chitosan hybrid microspheres and nanospheres for drug delivery. *The Journal of Physical Chemistry C*, 114(44), 18940–18945. <http://dx.doi.org/10.1021/jp105906p>
- Ye, J., Wang, D., Zeiger, D. N., Miles, W. C., & Lin-Gibson, S. (2013). Different kinetic pathways of early stage calcium-phosphate cluster aggregation induced by carboxylate-containing polymers. *Biomacromolecules*, 14(10), 3417–3422. <http://dx.doi.org/10.1021/bm400660a>
- Yusufoglu, Y., & Akinc, M. (2008). Effect of pH on the carbonate incorporation into the hydroxyapatite prepared by an oxidative decomposition of calcium-EDTA chelate. *Journal of the American Ceramic Society*, 91(1), 77–82. <http://dx.doi.org/10.1111/j.1551-2916.2007.02092.x>
- Yusufoglu, Y., Hu, Y., Kanapathipillai, M., Kramer, M., Kalay, Y. E., Thiagarajan, P., & Mallapragada, S. (2008). Bioinspired synthesis of self-assembled calcium phosphate nanocomposites using block copolymer-peptide conjugates. *Journal of Materials Research*, 23(12), 3196–3212. <http://dx.doi.org/10.1557/JMR.2008.0388>
- Zhang, Y., & Zhang, M. (2002). Calcium phosphate/chitosan composite scaffolds for controlled in vitro antibiotic drug release. *Journal of Biomedical Materials Research*, 62(3), 378–386. <http://dx.doi.org/10.1002/jbm.10312>